**Stallion Journal for Multidisciplinary Associated Research Studies**
ISSN (Online): 2583-3340
Volume-3 Issue-2 || April 2024 || PP. 25-35 https://doi.org/10.55544/sjmars.3.2.3

# Investigation the Gamma Ray Shielding Parameters for Portland Cement Doped with Several Metal Oxides

**Ali M. Ahmed[1], R. Y. J. AL-Salih[2] and Sabah Mahmoud Aman Allah Jaff[3]**
[1,2]Department of Physics, College of Science, University of Tikrit, Tikrit, IRAQ.
[3]Department of Physics, College of Education for Pure Science, University of Kirkuk, Kirkuk, IRAQ.

[1]Corresponding Author: lyly12876@gmail.com

**www.sjmars.com || Vol. 3 No. 2 (2024): April Issue**

| **Date of Submission:** 26-04-2023 | **Date of Acceptance:** 28-04-2024 | **Date of Publication:** 04-05-2024 |
|---|---|---|

**ABSTRACT**

**In this research, gamma ray photons emitted from radioactive sources (Cs-137, Ra-226) with energies (186, 242, 295, 352, 609, 662, 1120, 1765) keV, respectively, to study some parameters, Such as the linear attenuation coefficient ( $\mu_\ell$ ), mass attenuation coefficient ($\mu_m$ ) for shield made of composite materials consisting of cement as the base material reinforced with different materials (magnesium oxide MgO , tungsten oxide $WO_3$) nanoparticles with different reinforcement ratios (10, 30, 50) % and thickness (0.5) cm to protect against radiation. For this purpose, a sodium iodide detector activated with thallium NaI (T$l$)with dimensions ($1.5^{''} \times 1.5^{''}$) was used with an integrated measuring system, to determine the suitability of these shields for use in the field of gamma ray protection. The results showed that the values of these parameters are affected by changing the reinforcement ratios and the gamma ray energy. It was found that when increasing the reinforcement ratio of the shield led to an increase in the linear and mass attenuation coefficient, and in contrast, a decrease in the values of each occurs when the gamma ray energy of the used radioactive source is increased, especially at a concentration of 50 % and at energy (1765) Kev.**

***Keywords***- Gamma rays, Linear and Mass attenuation coefficient, Sodium Iodide Detector, Shielding.

## I. INTRODUCTION

When radiation passes through any material, its intensity gradually reduces as a result of a series of interactions. The linear attenuation coefficient µ, which is defined as the probability of a radiation interacting with a material per unit path length (Woods, 1982). it is the important quantity characterizing the penetration and diffusion of gamma radiation in a medium. The mass attenuation coefficient is essential parameter to derive several other parameters of shielding, radiation interaction and dosimetry and etc. It a measure of γ-rays absorption or scattering. The magnitude of attenuation coefficients depends on the incident photon energy, the atomic number and the density of the materials. Recently many researchers have been studied on determination of mass attenuation coefficients experimentally for different materials. A more detailed surveys and exhaustive list of references can be found in (Han and Demir, 2009). There are many ways to control external exposure to radiation and reduce it to a minimum, especially protective shields because they actually lead to safe practical levels. Although there are different materials used for shielding against gamma rays, lead comes first because it has a high confining power that helps reduce the thickness of armor made from it, However, due to the large areas required to be protected, especially when designing protective shields from gamma rays in hospitals, clinics, and nuclear facilities, the use of lead becomes expensive, and therefore concrete and other building materials are used to increase the thickness of the protective walls (Martin , 2012).

Therefore, research and studies continued to design protective shields from gamma rays with their high penetrating power, by knowing the attenuation coefficients of each material and knowing its ability to block these rays.

The attenuation coefficients of gamma rays were studied practically and theoretically in a number of materials such as sand, cement, bricks and others. Building materials used in Turkey, at the energy range of gamma ray (81- 1332) keV By researchers (Damla et al., 2012). The results have shown that Iraqi cement is one of the best building materials to be used in shielding against gamma rays with a mass attenuation coefficient of $0.252\ cm^2/\text{g}$ at photon energy of (81) keV . (Abd El – Latif et al.,2013 ) have Studied the linear and mass attenuation coefficients experimentally using cement, which is a base material for a composite material, which was reinforced with different proportions of iron slag (5 , 15 ,25 , 35 , 45 ) % the measurements were made using gamma rays from a point source (C0-60 , CS – 137 ) , The results showed that adding iron slag at a rate of 45% to the cement significantly increases the density of the overlay material, and this provides the best ability to attenuate radiation among other samples. Therefore, the reinforcement process contributes to a significant improvement in the shielding properties of gamma rays. (Ya Yao et al., 2016) also studied the shielding coefficients of bismuth oxide (Bi2o3) and lead oxide (Po) as an additive to concrete as a base material using a sodium iodide detector NaI (TI) and energy 662 MeV with different reinforcement ratios. They showed Results: Adding 25% bismuth oxide to concrete greatly increases the density of the composite material, and this provides the best ability to attenuate gamma ray photons. (Ali h. Taqi et al., 2017) have studied Mass attenuation coefficient for different building materials (Iraqi cement - Turkish cement - Iranian ceramics - Turkish ceramics - Spanish ceramics - Indian ceramics - Chinese ceramics - Iraqi gypsum) using a sodium iodide detector NaI (TI) and different energies (59.5, 356.5, 662, 1173, 1332) Kev. The results showed that Iraqi cement is the best building material for use in shielding against gamma rays.

The current research aims to find alternative materials for lead used as protective shields against gamma rays in the medical and research fields, which are of high density, have a large atomic number, are non-toxic, and are low in cost, and can be prepared in different shapes. Shields made of composite materials consisting of cement (as a base material) supported by various materials such as (Magnesium oxide MgO, tungsten oxide WO3) with different concentrations and a fixed thickness. The effect of the concentrations of supported materials on the behavior of some parameters such as the linear attenuation coefficient and the mass attenuation coefficient was studied using a sodium iodide detector NaI (Tl) with dimensions ($1.5'' \times 1.5''$) with an integrated measuring system and different energies (186, 242 , 295, 352, 609, 662, 1120, 1765) keV respectively, in addition to studying the effect of changing the energy of different gamma rays on these parameters and their behavior.

## II. THEORETICAL PART

The interaction of gamma radiation differs from the interaction of charged particles with matter. Gamma rays may be characterized in that they do not lose their energy suddenly and their penetration into matter is greater than in the case of charged particles penetrating matter because they are able to pass a distance inside it without interacting with its atoms (Turner et al., 2008), Therefore, we notice that when a beam of gamma ray photons incident towards a substance, the incident photons interact mainly with the atoms of this substance in one of the following ways (photoelectric phenomenon, Compton scattering, pair production) (Khan et al., 2014). In each of these interactions, there is a possibility of transferring part or all of the photon energy to one of the atomic electrons of the target material, and this all depends on the nature of the target material and the energy of the incident photon (Cottingham et al., 2001).

When a beam of gamma rays passes through a certain material, the photons of this beam either exit without interaction or are completely removed from the beam by the process of scattering or absorption. If there is a beam of intensity ($I_\circ$), incident on a material of thickness (x), then the intensity of the beam penetrating ($I_x$) through the material is given by the Beer-Lambert relationship, through which the linear attenuation coefficient is calculated (Al-saadi et al., 2014):-

$$\mathbf{I_x = I_\circ\, e^{-\mu x}} \qquad \ldots\ldots\ldots\ldots\ldots (1)$$

We note from equation (1) that the transmitting beam experienced an exponential decrease in intensity along the path (x) that it traveled. To apply the above equation, the gamma rays must be single-energy and narrow, and the thickness of the target material must be small (Akça et al., 2014).

The mass attenuation coefficient, which represents the linear attenuation coefficient divided by the density, was calculated using the following relationship:

$$\boldsymbol{\mu_m = \frac{\mu(cm^{-1})}{\rho}} \qquad \ldots\ldots\ldots\ldots\ldots (2)$$

Where: ρ is the density of the absorbent material)$\text{g/cm}^3$).

## III. PRACTICAL PART

The gamma ray counting system consists of the following parts, as shown in Figure (1):

 

**Stallion Journal for Multidisciplinary Associated Research Studies**
ISSN (Online): 2583-3340
Volume-3 Issue-2 || April 2024 || PP. 25-35 https://doi.org/10.55544/sjmars.3.2.3

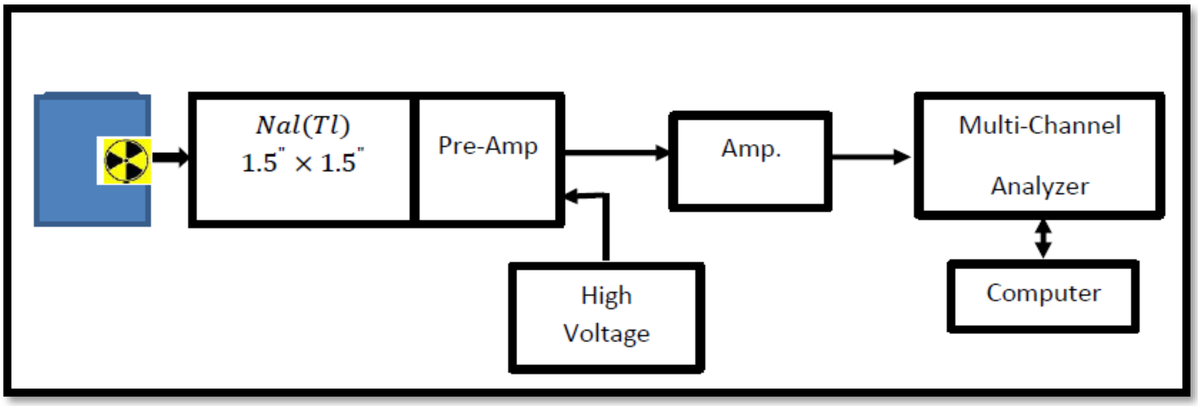


**Fig.1.** The electronic counting system used in the research.

***3-1 Scintillation Detector***

The detector used in this work is a radiation sensor, model 6S6P1.5VD, with dimensions (3.81 x 3.81) cm. The scintillation detector (6S6P1.5VD) is designed to be an X-ray and gamma ray detector, as well as it is versatile and suitable for many applications. Its size is small enough to be useful for low and medium photon energies from low energy sources but is also useful at much higher energies. It has a built-in internal voltage divider to allow simple and convenient operation of the device. The scintillator is a high-voltage positive detector that uses a 10 stage multiplexed phototube (PMT) attached to a cylindrical photonic crystal of sodium iodide doped with thallium NaI (Tl) with dimensions ($1.5^{"} \times 1.5^{"}$). The voltage divider is connected to the (PMT) inside the cover and the ground voltage divider is connected to the end of the cover, which is electrically connected to the outer cover, as in Figure (2).

**Fig.2.** Sodium iodide doped with thallium NaI (Tl).

***3-2 High Voltage Power Supply***

The voltage sensor is connected to sodium iodide doped with thallium NaI(Tl) to equip the base of the photomultiplier with voltages in a range of (0-1200) V, while the detector is equipped with a voltage of 700V.

***3-3 Optical multiplier base***

The photomultiplier base divides the supplied voltages from the high power supply to the photomultiplier diodes equally and is connected to series resistors in order to determine the path of the electrons.

***3-4 Pre-Amplifier***

The pulses collected in the detector are exited by the photomultiplier occurring in the photomultiplier tube and then enter the preamplifier or primary amplifier. The function of the amplifier is to receive the signal coming out of the detector and reduce the rate of electronic noise, thus preventing the pulses from overlapping one another. Then all of these pulses pass through Pulses, even pulses of small amplitude, until they reach the main amplifier or secondary amplifier.

***3-5 Secondary-Amplifier***

This amplifier contains an input and an output, and the input is connected to the output of the primary amplifier (Pre-Amplifier), and the output of the secondary amplifier is connected to the computer card, and the amplified pulses appear in the form of a spectrum directly in its program, and this amplifier is one of the basic parts in A system for

**Stallion Journal for Multidisciplinary Associated Research Studies**
ISSN (Online): 2583-3340
Volume-3 Issue-2 || April 2024 || PP. 25-35 https://doi.org/10.55544/sjmars.3.2.3

measuring and counting gamma rays using a thallium-activated sodium iodide detector. This contains a wide amplification key (Coarse Gain) as well as a fine amplification key (Fine Gain), through which the amplifier increases the amplitude ratio of the pulse entering the amplifier and connects it to the computer better.

***3-6 Integrated Computer Spectrometer***

The Integrated Computer Spectrometer (ICS) provides a unique solution for measuring nuclear spectrometry, using the basic computer system software. It contains a multi-channel analyzer (MCA) that is used to measure the distribution voltage, and thus the energy distribution of gamma reactions. It also contains many advanced features including a computer-linked amplifier and a high-voltage photomultiplier tube (PMT), High- and low-level distinctions, and data memory on the device. It is designed to work easily with a computer for stable operation and low noise. The microprocessor on the board acts as the main control device and data storage device, as shown in Figure (3).

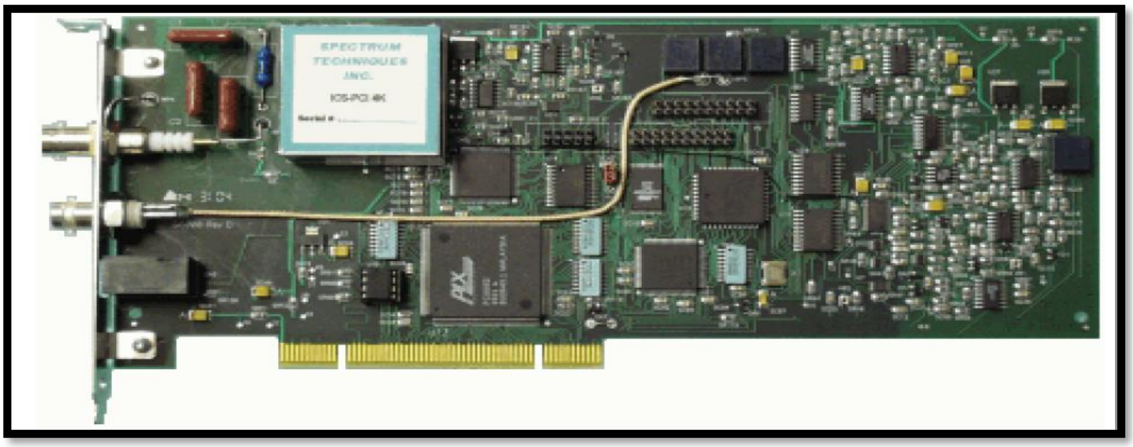

**Fig.3.** Integrated Computer Spectrometer (ICS).

The ADC configuration has a capacity of 1024 channels with a random timer and excellent data transfer capability at high counting rates with minimal time loss. The conversion gain may be changed from 1024, 512 or 256 channels, via software. In the current work the conversion gain was 1024. channel which is used to cover the power range studied (185–1765) keV as shown in the Amp / HV / ADC adjustment window of the program, shown in Figure (4).

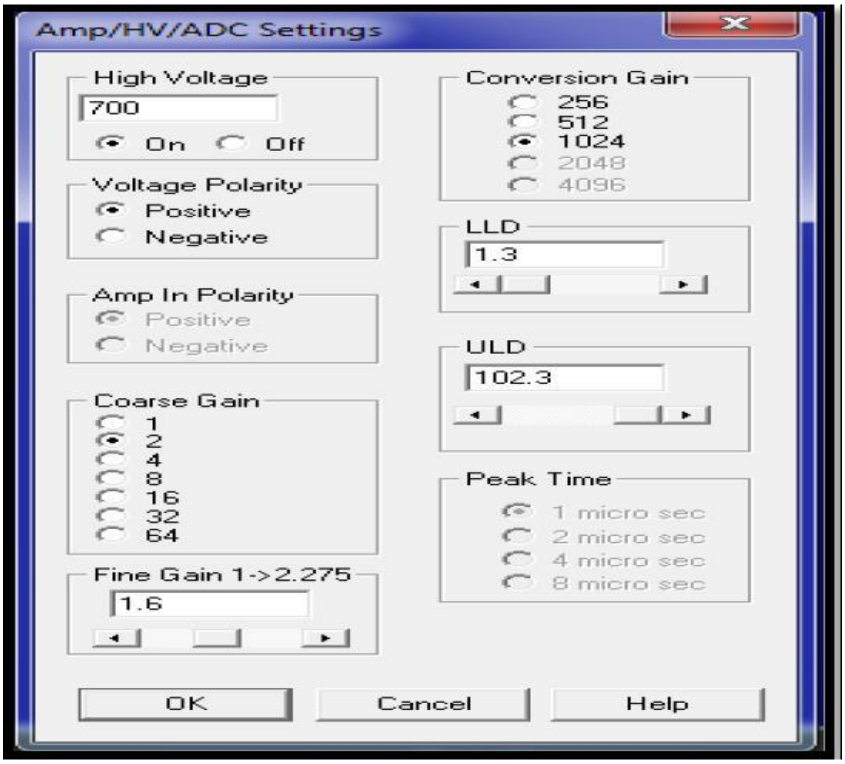


**Fig.4.** Adjustment window Amp/HV/ADC .

## IV. RADIATION SOURCES

In this research, two types of available sources are used:
1 - (Cs-137) Its effectiveness when measured is (188 kBq) and its half-life is (30.17 years). It was made in 1989 AD, with an efficiency of (400 kBq), which emits gamma rays with an energy of (662) keV.
2 - (Ra-266) Its effectiveness when measured is (1.97 KBq) and its half-life is (1600 years). It was made in 1989 AD, with an efficiency of (3 kBq), which emits gamma rays with energies (186, 242, 295, 352, 609, 1120, 1765) keV.

## V. SAMPLE PREPARATION

The shields (samples), details of which are shown in Table (1), were prepared in a special room for preparing samples by the following steps: -
1 - Preparing a plastic mold (cylindrical shape) with a thickness of (0.5) cm and a diameter of (2) cm. These molds were chosen to be suitable for the dimensions of the detector used and the collimators.
2 - A sensitive balance with a measurement accuracy of (0.001g) is used to weigh the base material (cement) according to the required volume fractions, which are placed in a dry glass beaker and ready for mixing.
3 - The volume of the plastic mold (cylindrical in shape) was calculated by the following relationship:

$$\mathbf{V = \pi r^2 h} \qquad \ldots\ldots\ldots\ldots\ldots\ldots \quad \mathbf{(3)}$$

Where: V ($cm^3$)is the volume of the mold , h (cm) is the height of the mold , r (cm) is the radius.
4 - The density of the samples was calculated using By equation:

$$\boldsymbol{\rho_{sample}} = \frac{\mathbf{m_s}}{\mathbf{V}} \qquad \ldots\ldots\ldots\ldots\ldots\ldots \quad (\mathbf{4})$$

Where: $\rho_{sample}$ $\left(\frac{g}{cm^3}\right)$ is the density of the sample , $m_s$ (g) is the mass of the sample , $V_s$ ($cm^3$)is the volume of the sample .
5 - Weigh the reinforcement material to be added using a sensitive balance with a measurement accuracy of (0.001g).
6 - Add the reinforcing material (magnesium oxide and tungsten oxide) in the glass beaker containing the cement. We stir the mixture using a glass tube until it is completely homogeneous to obtain the best mixture without gaps and bubbles. After that, the mixture is transferred to the mold designated for pouring, and then the mixture is left in the mold at room temperature. A secluded place until the hardening process is completed, which takes approximately 72 hours.
7 - Extracting the mold from the casting process in order to ensure the end of the interaction between the base material and the support material, thus obtaining high-hardness protective materials.

**Table 1. includes details of the samples according to the reinforcement material, the base material, and the reinforcement ratios of each.**

| **Sample code** | Base material | concentration | Reinforcement material | concentration |
|---|---|---|---|---|
| cement (pure) | Cement | 100 % | - | 0 |
| Group (1) | Cement | 90 % | MgO | 10 % |
| | | 70 % | | 30 % |
| | | 50 % | | 50 % |
| Group (2) | Cement | 90 % | $WO_3$ | 10 % |
| | | 70 % | | 30 % |
| | | 50 % | | 50 % |

## VI. RESULTS AND DISCUSSION

### *6-1 Linear attenuation coefficient(μ) .*

The linear attenuation coefficient (μ) was measured for all the prepared shields, the details of which are shown in Table (1). The linear attenuation coefficient (μ) was measured for all the prepared shields whose details are shown in Table (1), for different energies and for different concentrations. The results of these experimental measurements were summarized in Table (2), and a graph was drawn between the linear attenuation coefficient and the concentration of the reinforcement material added to The base material is as in Figures (5 and 6). We notice from this figure that the values of the linear attenuation coefficient for the samples change with changing concentration , It was noted that these values increase with the increase in the concentration of the added reinforcement material and for all energies, and this can be interpreted that when the concentration of the added reinforcement material increases, the attenuation processes in it will increase due to the increased distribution of the added reinforcement material within the base material, and leads to an increase in the density of the prepared samples in general. Thus, there is an increase in the attenuation of gamma rays. Therefore, the linear attenuation coefficient increases. We note that cement only is not suitable for use as a shield against gamma rays, but when the reinforcement material ($WO_3$, MgO) is added to it, the cement material becomes possible to use as a shield to attenuate gamma rays, and this behavior is consistent with (AL-Dhuhaibat et al., 2015).

A relationship was also drawn between the linear attenuation coefficient and energy, as in Figures (7 and 8). We notice from this figure that the linear attenuation coefficient decreases with the increase in the energy of the incident photons, and the reason for this is due to the difference in the mechanics of the interaction of gamma rays with sample with different energy values used. According to these figures, we notice that the values of the linear attenuation coefficient increase in the low power region, and this is consistent with (MD. hossai Sahadath et al., 2016) , this can be explained on the basis of the dominance of the effect of the photoelectric phenomenon, whose cross-section is high within this region. We notice by increasing the energy that Compton scattering is the most influential, so the attenuation coefficient decreases slowly up to the high energy range in which the effect of the pair production phenomenon dominates the reaction process and there is no noticeable change in the values of the linear attenuation coefficient within this region.

**Table 2. Linear attenuation coefficients (μ) in units of ($cm^{-1}$).**

| **Sample code** | **concentration** | E (keV) | | | | | | | |
|---|---|---|---|---|---|---|---|---|---|
| | | **186** | **242** | **295** | **352** | **609** | **662** | **1120** | **1765** |
| | | **Ra-226** | | | | | **Cs-137** | **Ra-226** | |
| | | $\mu_\ell\,(cm^{-1})$ | | | | | | | |
| Cement (pure) | 100% | 0.3192 | 0.2753 | 0.2468 | 0.2243 | 0.1689 | 0.1620 | 0.1265 | 0.1041 |
| Group (1) | 10% | 0.3637 | 0.3136 | 0.2812 | 0.2556 | 0.1924 | 0.1846 | 0.1441 | 0.1186 |
| | 30% | 0.4016 | 0.3463 | 0.3105 | 0.2822 | 0.2125 | 0.2039 | 0.1591 | 0.1309 |
| | 50% | 0.4424 | 0.3815 | 0.3420 | 0.3109 | 0.2340 | 0.2245 | 0.1752 | 0.1442 |
| Group (2) | 10% | 0.6321 | 0.5451 | 0.4888 | 0.4442 | 0.3344 | 0.3209 | 0.2504 | 0.2061 |
| | 30% | 0.6853 | 0.5910 | 0.5299 | 0.4816 | 0.3626 | 0.3479 | 0.2715 | 0.2234 |
| | 50% | 0.7861 | 0.6779 | 0.6078 | 0.5524 | 0.4159 | 0.3990 | 0.3114 | 0.2563 |

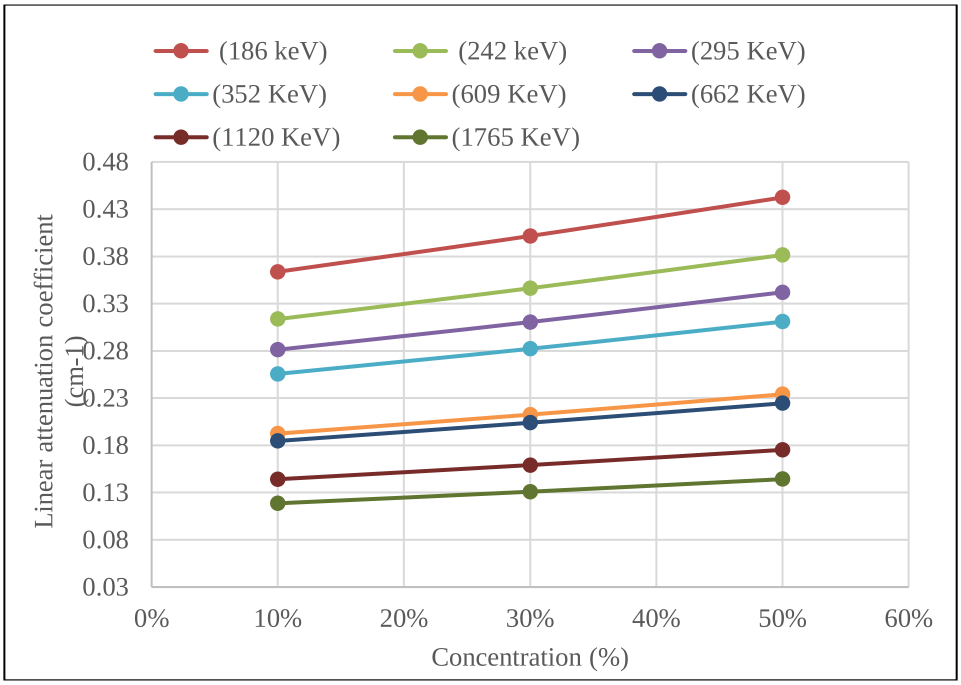


**Fig.5. The relationship of the linear attenuation coefficient to the concentration of the reinforcement material for different energies of shields of shields Group (1).**

**Stallion Journal for Multidisciplinary Associated Research Studies**
ISSN (Online): 2583-3340
Volume-3 Issue-2 || April 2024 || PP. 25-35 https://doi.org/10.55544/sjmars.3.2.3

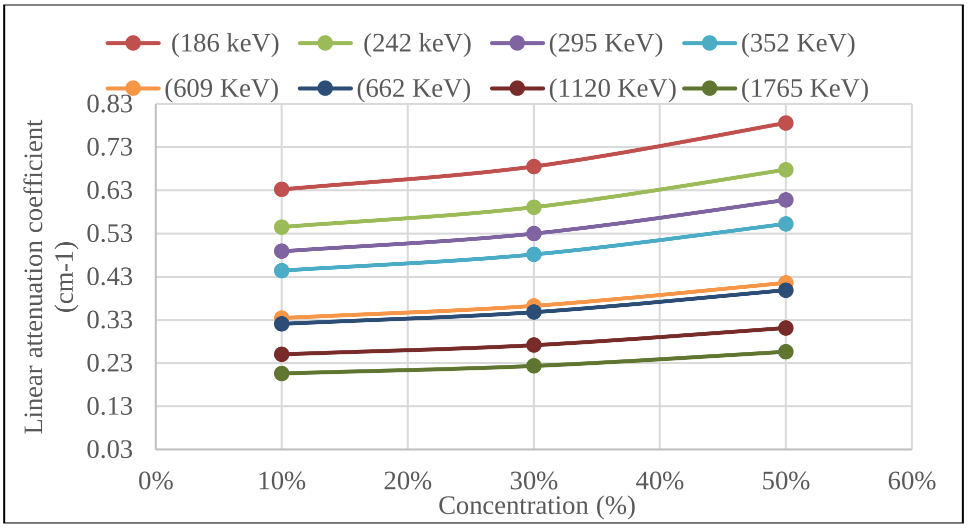


**Fig.6. The relationship of the linear attenuation coefficient to the concentration of the reinforcement material for different energies of shields Group (2).**

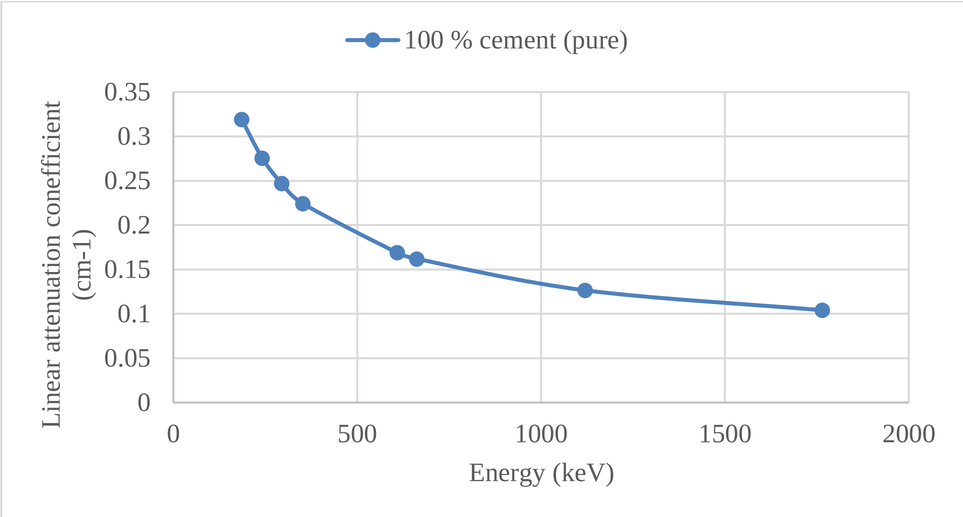


**Fig.7. The relationship of the linear attenuation coefficient to the energy of the incident photon for the cement material 100%.**

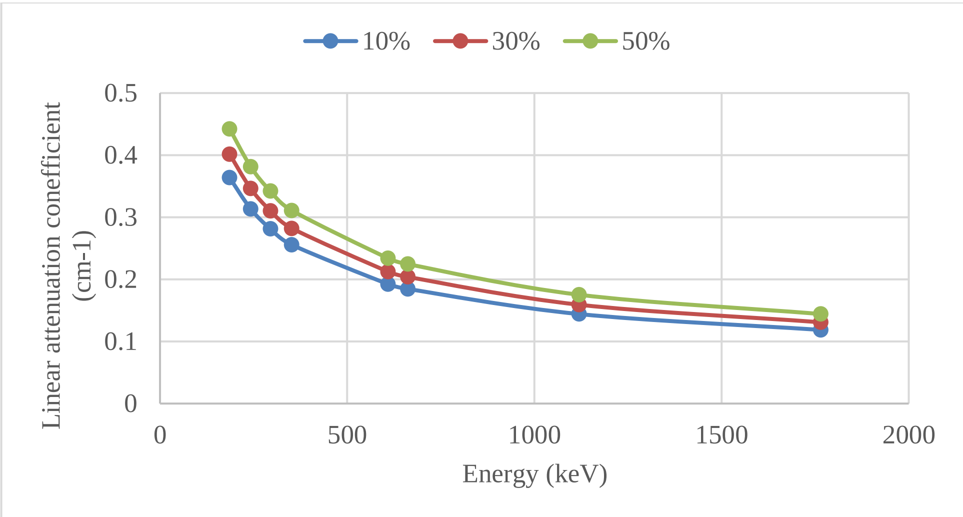


**Fig.8. The relationship of the linear attenuation coefficient to the energy of the incident photon for different concentrations of shields Group (1).**

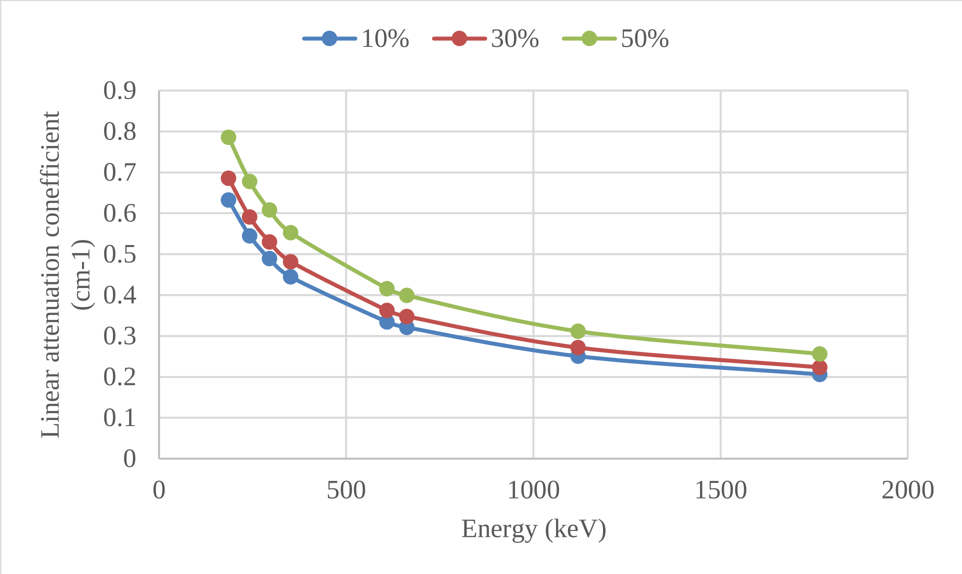


**Fig.9. The relationship of the linear attenuation coefficient to the energy of the incident photon for different concentrations of shields Group (2).**

***6- 2 Mass attenuation coefficient($\mu_m$).***

The mass attenuation coefficient ($\mu_m$) was calculated from equation (2) for all shields, with different energies and different concentrations, the results of these calculations were written in Table (3). The relationship between the mass attenuation coefficient and the concentration of the reinforcement material was drawn as in Figures (10 and 11) , We notice from these figures that the values of the mass attenuation coefficient of shields change with changing concentration, as it is clear that these values increase with increasing concentration of the reinforcement material , this is because the values of the linear attenuation coefficient increase slightly when the concentration increases, while the density increases with increasing concentration, which affects the values of the mass attenuation coefficient.

We note that the use of some materials such as (magnesium oxide and tungsten oxide) added to the base material has a direct effect on the value of the mass attenuation coefficient, and this is consistent with (Pawel et al., 2019). A relationship has been drawn between the mass attenuation coefficient and energy, as shown in Figures (12-14). We notice from these figures that the mass attenuation coefficient depends on energy, as it decreases with increasing energy, and this is due to the fact that when the photon energy is between (100 keV) and (10 MeV) the Compton scattering process becomes the dominant mechanism, so that we notice that the mass attenuation coefficient slowly decreases with increasing photon energy, we notice that the mass attenuation coefficient decreases slowly with increasing photon energy. Because the cross section of the Compton scattering process is inversely proportional to the energy of the photons, and this is consistent with (Tekin et al., 2017).

**Table 3. Mass attenuation coefficients ( $\mu_m$) in units of ($cm^2/gm$).**

| Sample code | concentration | E (keV) | | | | | | | |
|---|---|---|---|---|---|---|---|---|---|
| | | 186 | 242 | 295 | 352 | 609 | 662 | 1120 | 1765 |
| | | Ra-226 | | | | | Cs-137 | Ra-226 | |
| | | $\mu_m$ ($cm^2/gm$) | | | | | | | |
| Cement (pure) | 100% | 0.1388 | 0.1197 | 0.1073 | 0.0975 | 0.0734 | 0.0705 | 0.0550 | 0.0453 |
| Group (1) | 10% | 0.1527 | 0.1317 | 0.1180 | 0.1073 | 0.0808 | 0.0775 | 0.0605 | 0.0498 |
| | 30% | 0.1638 | 0.1412 | 0.1266 | 0.1151 | 0.0866 | 0.0831 | 0.0649 | 0.0534 |
| | 50% | 0.1763 | 0.1520 | 0.1363 | 0.1239 | 0.0933 | 0.0895 | 0.0698 | 0.0575 |
| Group (2) | 10% | 0.2276 | 0.1963 | 0.1760 | 0.1600 | 0.1204 | 0.1155 | 0.0902 | 0.0742 |
| | 30% | 0.2360 | 0.2035 | 0.1824 | 0.1658 | 0.1248 | 0.1198 | 0.0935 | 0.0769 |
| | 50% | 0.2498 | 0.2154 | 0.1932 | 0.1756 | 0.1322 | 0.1268 | 0.0990 | 0.0815 |

**Stallion Journal for Multidisciplinary Associated Research Studies**
ISSN (Online): 2583-3340
Volume-3 Issue-2 || April 2024 || PP. 25-35 https://doi.org/10.55544/sjmars.3.2.3

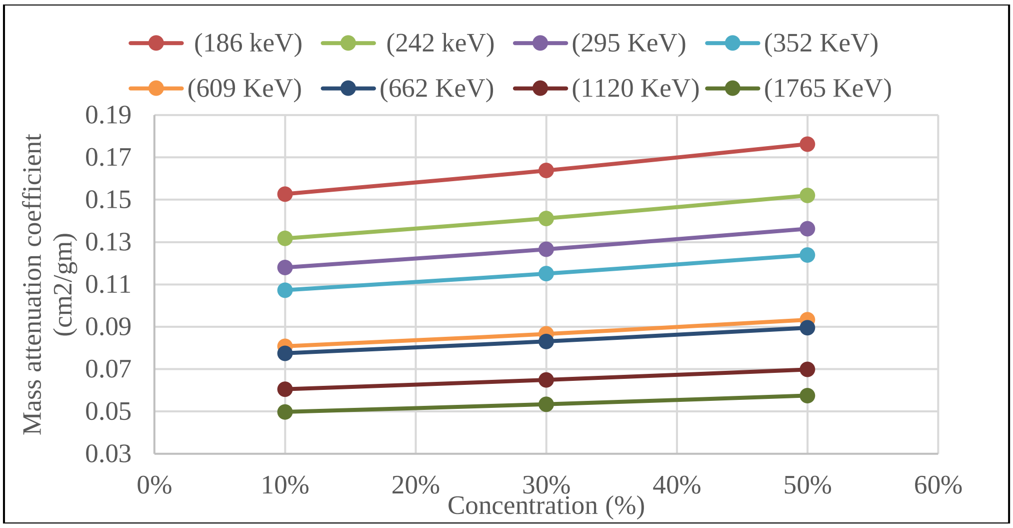


**Fig.10. The relationship of the mass attenuation coefficient to the concentration of the reinforcement material for different energies of shields of shields Group (1).**

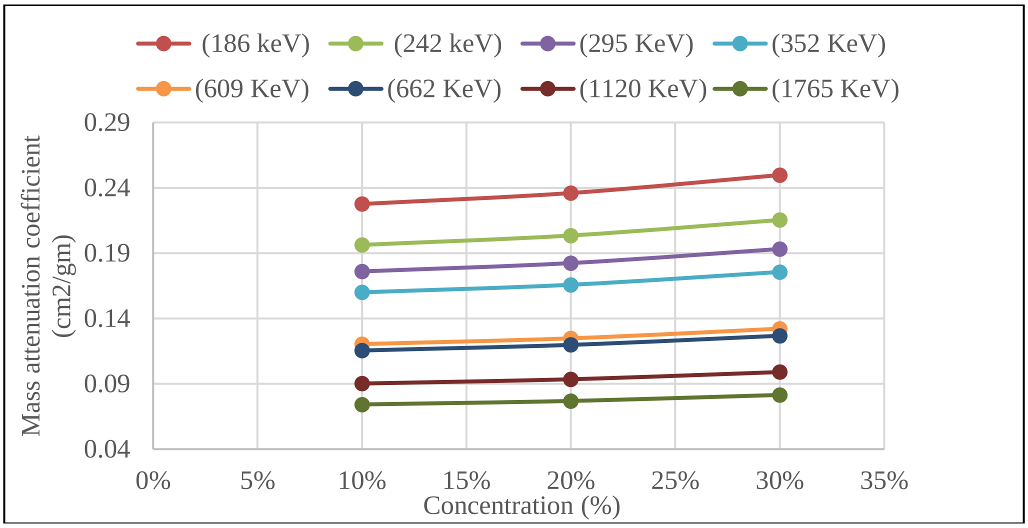


**Fig.11. The relationship of the mass attenuation coefficient to the concentration of the reinforcement material for different energies of shields of shields Group (2).**

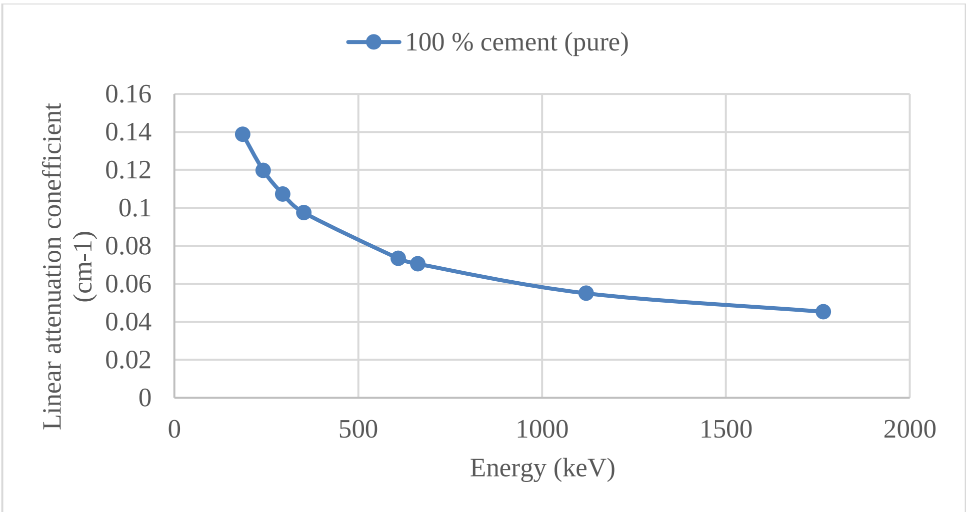


**Fig.12. The relationship of the mass attenuation coefficient to the energy of the incident photon for the cement material 100%.**

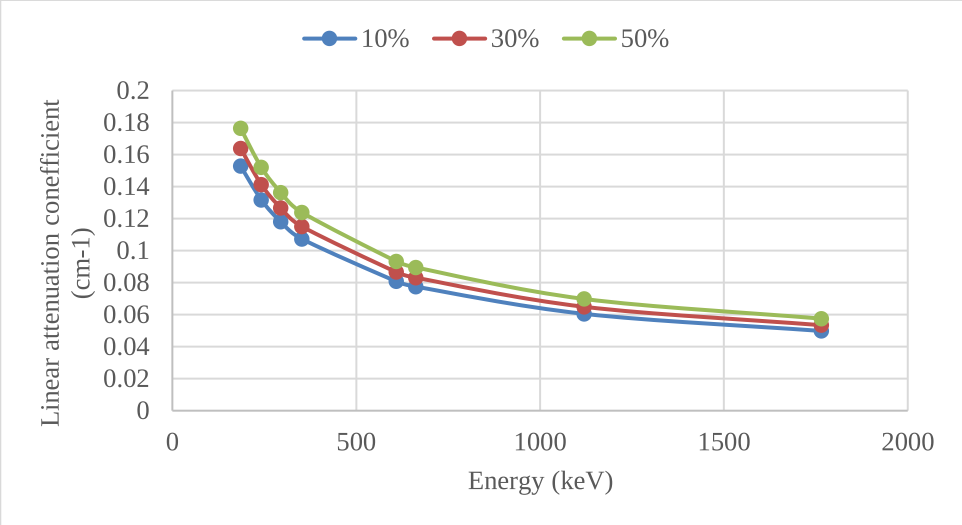


**Fig.13. The relationship of the mass attenuation coefficient to the energy of the incident photon for different concentrations of shields Group (1).**

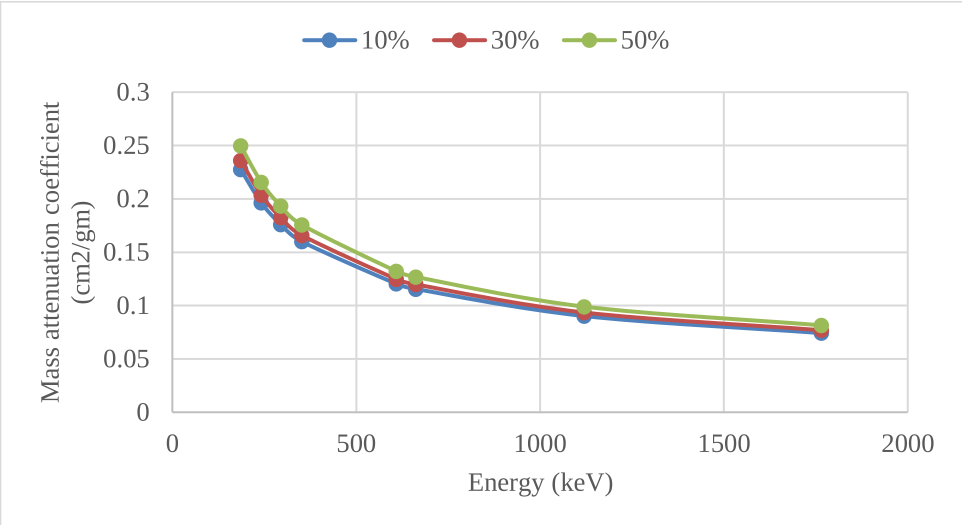


**Fig.14. The relationship of the mass attenuation coefficient to the energy of the incident photon for different concentrations of shields Group (2).**

## VII. CONCLUSION

1- By using composite materials (cement + oxides), it is possible to form shields with a high ability to attenuate radiation and replace high-cost materials with less expensive materials.
2- The results showed that there is a difference in behavior between the linear and mass attenuation coefficient.
3- The linear and mass attenuation coefficient increase with increasing concentration of the doped material and decrease with increasing gamma ray energy.
4- The attenuation coefficients of gamma rays are affected by the density of the target material.
5- The shielding properties of gamma rays were improved by using cement and some doped materials in certain proportions, these shields could be used in some future nuclear applications such as radiotherapy rooms and radiation containers.

## REFERENCES

[1] Woods, J., 1982. Computational Methods in Reactor Shielding. Pergamon Press, New York.
[2] Han, I., Demir, L., 2009. Determination of mass attenuation coefficients, effective atomic and electron numbers for Cr ,Fe and Ni alloys at different energies. Nucl. Instrum. Methods Phys. Res. B 267, 3–8.

[3] Damla, B.H.; Celik, A.; Kiris, E.; Cevik, U. (2012). Calculation of radiation attenuation
[4] coefficient affective atomic number and electron densities for some building materials .
[5] Radiation Protection Dosimetry, 150(4), 541–549.
[6] Abd El-Latif Abd El-Ghany Abd El-Latif Ahmed 1, Khalifa S. Saeid2, H.S. Ragab1 and A.A. Abdalla2" Effect of Gamma Ray Energies and Addition of Iron Slag by weight to Portland Cements on Mass Attenuation Coefficient" , Journal of Materials Science and Engineering , A 3 (12) 838-842 , p.839-842 , (2013).
[7] Ya Yao, Xiaowen Zhang, Mi Li, Rong Yang, Tianjiao Jiang, Junwen Lv," Investigation of Gama ray shielding efficiency and mechanical performances of concrete shields containing bismuth oxide as an environmentally friendly additive" , Radiation Physics and Chemistry,(16), p.30203,(2016).
[8] Ali H. Taqi, Hero J. Khalil" Experimental and Theoretical Investigation of Gamma Attenuation of Building Materials" , Journal of Nuclear and Particle Physics, 7(1), p. 6-13, (2017).
[9] Turner, J. E. "Atoms, radiation, and radiation protection ", 3rd edn. John Wiley & Sons .(2008) ,
[10] Khan, F. M., & Gibbons, J. P. "Khan's the physics of radiation therapy ", 5th edn. Lippincott Williams & Wilkins, (2014).
[11] Cottingham, W. N., Greenwood, D. A., & Greenwood, D. A. "An introduction to nuclear physics", 2nd edn. Cambridge University Press, (2001).
[12] Al-Saadi, A. J., & Saadon, A. K. "Gamma Ray Attenuation Coefficients for Lead Oxide and Iron Oxide Reinforced in Silicate Glasses as Radiation Shielding Windows", Ibn AL-Haitham Journal for Pure and Applied Science, 27(3), p.201-214, (2014).
[13] Akça, B., & Erzeneoğlu, S. Z. "The mass attenuation coefficients, electronic, atomic, and molecular cross sections, effective atomic numbers, and electron densities for compounds of some biomedically important elements at 59.5 keV", Science and Technology of Nuclear Installations, 2014, (2014).
[14] MD. Hossain Sahadath, Ripan Biswas, MD. Fazlulhuq And Abdus Sattar Mollah. " Calculation Of Gamma-ray Attenuation Parameters For Locally Developed Ilmenite -Magnetite Concrete", J. Bangladesh Acad. Sci, 40, (1), p.11-21.(2016) ,
[15] AL-Dhuhaibat, M. J. "Study of the shielding properties for some composite materials manufactured from polymer epoxy supported by cement, aluminum, iron and lead against gamma rays of the cobalt radioactive source (Co-60) ", International Journal of Application or Innovation in Engineering & Management, 4(6), p. 90-98, (2015).
[16] Pawel Sikora a, Mohamed Abd Elrahman b,c, Elzbieta Horszczaruk a, Piotr Brzozowski a, Dietmar Stephan ," Incorporation of magnetite powder as a cement additive for improving thermal resistance and gamma-ray shielding properties of cement-based composites" , Construction and Building Materials, 204,p. (2019), 113–121.
[17] Tekin, H. O., Singh, V. P., & Manici, T. "Effects of micro-sized and nano-sized WO3 on mass attenauation coefficients of concrete by using MCNPX code", Applied Radiation and Isotopes,121, p. 122-125, (2017).